HHS Public Access

Author manuscript

Biochemistry. Author manuscript; available in PMC 2020 February 05.

Published in final edited form as:

Biochemistry. 2000 January 11; 39(1): 86–91. doi:10.1021/bi991903b.

Inhibitory Region of Troponin I: Ca^{2+}-Dependent Structural and Environmental Changes in the Troponin–Tropomyosin Complex and in Reconstituted Thin Filaments

Tomoyoshi Kobayashi[‡], **Minae Kobayashi**[‡], **Zygmunt Gryczynski**[‡], **Joseph R. Lakowicz**[‡,§], **John H. Collins**[*,‡,§]

Medical Biotechnology Center, University of Maryland Biotechnology Institute, Baltimore, Maryland 21201, and Department of Biochemistry and Molecular Biology, University of Maryland School of Medicine, Baltimore, Maryland 21201

Abstract

In muscle thin filaments, the inhibitory region (residues 96–117) of troponin I (TnI) is thought to interact with troponin C (TnC) in the presence of Ca^{2+} and with actin in the absence of Ca^{2+}. To better understand these interactions, we prepared mutant TnIs which contained a single Cys-96 or Cys-117 and labeled them with the thiol-specific fluorescent probe *N*-(iodoacetyl)-*N*′-(1-sulfo-5-naphthyl)ethylenediamine (IAEDANS). We characterized the microenvironments of the AEDANS labels on TnI in the presence and absence of Ca^{2+} by measuring the extent of acrylamide quenching of fluorescence and lifetime-resolved anisotropy. In the troponin–tropomyosin (Tn–Tm) complex, the AEDANS labels on both Cys-96 and Cys-117 were less accessible to solvent and less flexible in the presence of Ca^{2+}, reflecting closer interactions with TnC under these conditions. In reconstituted thin filaments, the environment of the AEDANS on Cys-96 was not greatly affected by Ca^{2+}, while the AEDANS on Cys-117 was more accessible but significantly less flexible as it moved away from actin and interacted strongly with TnC in the presence of Ca^{2+}. We used fluorescence resonance energy transfer (FRET) to measure distances between AEDANS on TnI Cys-96 or Cys-117 and 4-{[(dimethylamino)phenyl]azo}phenyl-4′-maleimide (DABmal) on actin Cys-374 in reconstituted thin filaments. In the absence of Ca^{2+}, the mean distances were 40.2 Å for Cys-96 and 35.2 Å for Cys-117. In the presence of Ca^{2+}, Cys-96 moved away from actin Cys-374 by ~3.6 Å, while Cys-117 moved away by ~8 Å. This suggests the existence of a flexible “hinge” region near the middle of TnI, allowing amino acid residues in the N-terminal half of TnI to interact with TnC in a Ca^{2+}-independent manner, while the C-terminal half of TnI binds to actin in the absence of Ca^{2+} or to TnC in the presence of Ca^{2+}. This is the first report to demonstrate structural movement of the inhibitory region of TnI in the thin filament.

The muscle thin filament proteins troponin (Tn)[1] and tropomyosin (Tm) regulate contraction invertebrate striated muscle by conferring Ca^{2+} sensitivity to the interaction of actin with myosin in the thick filaments. Tn is composed of three subunits: the Ca^{2+}-binding subunit

[*]To whom correspondence should be addressed: Medical Biotechnology Center, University of Maryland Biotechnology Institute, Baltimore, MD 21201. Telephone: (410) 706-8102. Fax: (410) 706-7364. collins@umbi.umd.edu.

[‡]University of Maryland Biotechnology Institute.

[§]University of Maryland School of Medicine.

TnC, the inhibitory subunit TnI, and the Tm-binding subunit TnT (for reviews, see refs 1–5). Little is known about the three-dimensional structures of TnI and TnT, and much remains to be learned about details of Tn subunit interactions with each other, Tm, and actin. A short segment of TnI (residues 96–117) comprises an inhibitory region which, like whole TnI, binds to actin and inhibits actomyosin ATPase activity in the absence of Ca^{2+}. This inhibition can be reversed by TnC in the presence of Ca^{2+} (6). Further studies showed that the N-terminal part of the TnI inhibitory region interacts with TnC, while the C-terminal half of the inhibitory region interacts with actin (7, 8). Thus, Ca^{2+}-dependent interactions between the inhibitory region of TnI and either actin or TnC are central to the Ca^{2+}-dependent regulation of muscle contraction. The crystal structure of vertebrate fast skeletal muscle TnC shows a dumbbell-shaped molecule with two globular domains, each of which contains a pair of Ca^{2+}-binding sites (9, 10). The sites in the N-terminal domain are regulatory and Ca^{2+}-specific, while the sites in the C-terminal domain bind both Ca^{2+} and Mg^{2+} and play a structural role. Binding of Ca^{2+} to the regulatory sites induces localized conformational changes which result in the exposure of a hydrophobic pocket in the N-terminal domain. This pocket interacts with a segment of TnI (residues 115–131) which overlaps with the C-terminal part of the TnI inhibitory region (11, 12).

The aim of this study is to characterize Ca^{2+}-dependent interactions of the inhibitory region of TnI with actin and TnC. We prepared single thiol mutants of TnI which contained either Cys-96 or Cys-117 at either end of the inhibitory region, and labeled them with the fluorescent probe 1,5-IAEDANS. We characterized the microenvironments of the AEDANS labels by measuring the extent of acrylamide quenching of fluorescence and lifetime-resolved anisotropy. We also labeled Cys-374 of actin with DABmal, and used FRET to measure distances between AEDANS and DABmal in reconstituted thin filaments.

EXPERIMENTAL PROCEDURES

Proteins.

Cys-less TnC (ΔCTnC), in which Cys-98 was replaced with Leu, and two single Cys mutants of TnI (Cys-96 and Cys-117) were expressed and purified as described previously (13, 14). TnT (15), Tm (16), and actin (17) were prepared from rabbit fast skeletal muscle according to previously described methods.

Labeling of TnI and Actin.

The single Cys residues of TnI-(Cys-96) and TnI(Cys-117) were labeled with 1,5-IAEDANS as described previously (13). The stoichiometry of labeling was 0.60–0.85 mol/mol. Labeling of Cys-374 of actin with DABmal was carried out as described by Tao et al. (18). Reaction times were varied to obtain labeling stoichiometries between 0.47 and 0.90. The substoichiometric labeling yields for the various samples were taken into account when calculating energy transfer efficiencies.

[1]Abbreviations: CNBr, cyanogen bromide; DABmal, 4-{[(dimethylamino) phenyl]azo}phenyl-4′-maleimide; EGTA, ethylene glycol bis-(2-aminoethyl ether)tetraacetic acid; FRET, fluorescence resonance energy transfer; HEPES, *N*-(2-hydroxyethyl)piperazine-*N*′-2-ethanesulfonic acid; IAEDANS, *N*-(iodoacetyl)-*N*′-(1-sulfo-5-naphthyl)ethylenediamine; Tm, tropomyosin; Tn, troponin.

Functional Characterization of Mutant and Labeled Proteins.

Previously described methods (13) were used to show that the mutant and labeled TnIs used in this study retained the Ca^{2+}-dependent ability of TnI to regulate actomyosin ATPase activity in a fully reconstituted system. DABmal-labeled actin has been widely used, and it has been established that it has retained its biological activity (e.g., ref 18).

Reconstitution of the Tn–Tm Complex and Thin Filaments.

Reconstitution and purification of the ternary complex of Tn from ΔCTnC, TnT, and labeled or unlabeled TnI(Cys-96) or TnI(Cys-117) were carried out as described previously (19). After Mono-Q column purification of the reconstituted Tn complex, equimolar amounts of Tn and Tm were combined and dialyzed against 0.3 M NaCl, 5 mM $MgCl_2$, 0.5 mM EGTA, and 10 mM HEPES (pH 7.5). To reconstitute thin filaments, the Tn–Tm complex was mixed with labeled or unlabeled F-actin and phalloidin in a molar ratio of 1:7: 14. The concentration of the Tn–Tm complex ranged from 0.7 to 1.0 *μM.* The mixture was then dialyzed against 0.1 M NaCl, 5 mM $MgCl_2$, 0.5 mM EGTA, and 10 mM HEPES (pH 7.5). Phalloidin was included because it is a well-known stabilizer of actin filaments. Although phalloidin does somewhat reduce the flexibility of actin filaments (20), it does not alter cooperative interactions among thin filament proteins (21).

Steady-State Fluorescence Measurements.

Steady-state fluorescence spectral measurements were carried out using an Instruments S. A. FluoroMax-2 spectrometer (JOBIN YBON-SPECS). All the measurements were carried out at 25 °C.

Acrylamide Quenching Experiments.

The Tn–Tm complex with AEDANS at Cys-96 or Cys-117 of TnI in 0.3 M NaCl containing 5 mM $MgCl_2$, 10 mM HEPES (pH 7.5), and either 0.1 mM $CaCl_2$ (in the presence of Ca^{2+}) or 0.5 mM EGTA (in the absence of Ca^{2+}) was titrated with freshly prepared 7.6 M acrylamide in the same solution. The same conditions were used for the reconstituted thin filaments, except that 0.1 M instead of 0.3 M NaCl was used.

Lifetime-Resolved Anisotropy Measurements.

The theory for the recovery of limiting anisotropy by lifetime-resolved anisotropy (or quenching-resolved emission anisotropy) measurements has been described in detail (22–24). Briefly, the measurement of anisotropy reveals the rotational displacement of the fluorophore during the period of the excited state, i.e., the lifetime τ. Decreasing the length of the duration of the excited state results in a higher steady-state anisotropy. If the correlation time for motion of the label within the protein, ϕ_L, is much shorter than the correlation time of overall protein motion, ϕ_P, i.e. $\phi_L \ll \phi_P$, the extent of the segmental motions of fluorophore can be estimated from r_0, the anisotropy in the absence of rotational diffusion, and $r(0)$, the anisotropy at $\tau = 0$.

$$1/r = 1/[r_0(1-\alpha_r)] + [\tau/r_0(1-\alpha_r)\phi_p] \quad (1)$$

where α_r is the fraction of the anisotropy which is lost by segmental motion. A plot of $1/r$ versus τ will be linear, and one can obtain $1/r(0)$ from the intercept at $\tau = 0$ on the $1/r$ axis. With a known value of r_0, one can use $r(0) = r_0(1 - \alpha_r)$ to calculate the average angular displacement of segmental motion with the following equation:

$$r(0)/r_0 = (3\left\langle \cos^2\theta \right\rangle - 1)/2 = 1 - \alpha_r \tag{2}$$

Mean lifetimes were calculated with (32)

$$\left\langle \tau \right\rangle = \sum(\alpha_i \tau_i^2)/\sum(\alpha_i \tau_i) \tag{3}$$

and lifetimes in the presence of quencher were obtained from the Stern–Volmer relationship.

$$\tau = \tau_0/(1 + K_{sv}[\text{quencher}]) \tag{4}$$

where τ_0 is the lifetime in the absence of quencher, K_{sv} is the Stern—Volmer constant, and [quencher] is the molar concentration of acrylamide. The steady-state anisotropy, r, of the fluorescence was measured as

$$r = (I_{VV} - I_{VH}G)/(I_{VV} + 2I_{VH}G) \tag{5}$$

where I_{VV} and I_{VH} are the vertical (parallel) and horizontal (perpendicular) components, respectively, of the emitted light when excited with vertically polarized light. The factor G is defined as I_{HV}/I_{HH}, where I_{HV} and I_{HH} are the vertical and horizontal components, respectively, of the emission when horizontally polarized excited light was used. The anisotropy in the absence of rotational diffusion, r_0, for 1,5-IAEDANS when excited at 370 nm was taken to be 0.35 (26).

Energy Transfer Measurements.

In these experiments, we used AEDANS-labeled Cys-96 or Cys-117 of TnI as a donor and DABmal-labeled Cys-374 of actin as an acceptor. To obtain the Förster critical distance, R_0, at which the energy transfer is 50% complete, we first measured the quantum yield, Q, of AEDANS in the thin filament, using quinine bisulfate as a standard ($Q = 0.55$ in 0.1 M H_2SO_4). The spectral overlap integrals, J, of the donor emission spectra and the acceptor absorbance spectra in the thin filaments were calculated as

$$J = \int_0^\infty \mathrm{Fd}(\lambda)\epsilon(\lambda)\lambda^4 \mathrm{d}\lambda \tag{6}$$

where Fd(λ) is the normalized fluorescence spectrum, defined as

$$\mathrm{Fd}(\lambda) = F(\lambda)/\int_0^\infty F(\lambda)\mathrm{d}\lambda \tag{7}$$

and $\epsilon(\lambda)$ is the absorbance spectrum of the acceptor expressed in M^{-1} cm^{-1}. Absorbance spectra were recorded using a JASCO V-550 spectrophotometer. J was numerically integrated at 1 nm intervals. R_0 (in angstroms) was then calculated from

$$R_0^6 = (8.79 \times 10^{-5})\eta^{-4} Q J \kappa^2 \quad (8)$$

where η is the refractive index and Q is the quantum yield of the donor in the absence of the acceptor.

Fluorescence lifetimes were measured using a frequency domain 10 GHz fluorometer equipped with a Hamamatsu 6 μm microchannel plate detector, as described previously (27). A pyridine II dye laser was used to excite AEDANS at 370 nm. Sample emission was filtered through an interference filter centered at 500 nm.

RESULTS

Acrylamide Quenching.

Acrylamide is a polar, uncharged compound that has been shown to quench the fluorescence of intrinsic tryptophan (28) or an extrinsic probe such as AEDANS (29). We used acrylamide as a quencher to measure Stern–Volmer quenching constants (K_{sv}) of our AEDANS fluorophores in both the Tn–Tm complex and reconstituted thin filaments, in the presence and absence of Ca^{2+} (Figure 1). We obtained quenching rate constants (k_q) from the K_{sv} and the mean lifetimes according to

$$k_q = K_{sv} / \langle \tau \rangle \quad (9)$$

and the results are summarized in Table 1. The k_q value for TnI Cys-96 in reconstituted thin filaments was the same in both the presence and absence of Ca^{2+}, while in all other cases we obtained reproducible Ca^{2+}-dependent changes of 10–26%. Ca^{2+}-dependent changes in k_q values (see Table 1) show that the effects of Ca^{2+} on the quenching of AEDANS fluorescence differed between the Tn–Tm complex and reconstituted thin filaments. In the Tn–Tm complex, AEDANS labels at both Cys-96 and Cys-117 were less exposed to the acrylamide quencher in the presence of Ca^{2+}, as shown by lower K_q values. In reconstituted thin filaments, on the other hand, AEDANS at TnI Cys-117 was more exposed to quencher (higher K_q) in the presence of Ca^{2+}, while Ca^{2+} had no effect (unchanged K_q) on the accessibility of AEDANS at TnI Cys-96. Our K_q measurements were precise within a standard deviation of ±0.01, so the differences we observed are statistically significant.

Lifetime-Resolved Anisotropy of AEDANS at TnI Cys-96 and TnI Cys-117.

We also examined the flexibilities of the AEDANS labels on TnI by measuring their lifetime-resolved anisotropies in Tn–Tm complexes and reconstituted thin filaments in the presence and absence of Ca^{2+}. As shown in Figure 2, plots of $1/r$ versus τ are linear. From the extrapolated intercepts at $\tau = 0$ on the $1/r$ axis, we obtained limiting anisotropy values, $r(0)$, which are listed in Table 1. In the Tn–Tm complexes, there is little difference between the flexibilities of AEDANS labels on Cys-96 and Cys-117. In reconstituted thin filaments, $r(0)$ values are higher for Cys-117 than for Cys-96, showing that the AEDANS on TnI

Cys-117 is less flexible than the AEDANS on TnI Cys-96. The flexibilities of the two AEDANS labels were affected by Ca^{2+} in different ways. For TnI Cys-117, in both the Tn–Tm complex and reconstituted thin filaments, higher $r(0)$ values show that the AEDANS label is less flexible in the presence of Ca^{2+}. For TnI Cys-96 in the Tn–Tm complex, a decreased flexibility in the presence of Ca^{2+} is also seen, although the difference is smaller than for Cys-117. For TnI Cys-96 in the reconstituted thin filaments, on the other hand, a lower $r(0)$ value shows that the AEDANS label is somewhat more flexible in the presence of Ca^{2+}. We used the $r(0)$ values to calculate minimum and maximum R values (R_{min} and R_{max}, respectively) as discussed below (see Table 2).

Effects of Ca^{2+} on Distances between TnI and Actin.

We used AEDANS-labeled Cys-96 or Cys-117 of TnI as a donor and DABmal-labeled Cys-374 of actin as an acceptor to obtain distances in reconstituted thin filaments. The overlap integrals, J, of donor fluorescence spectra and acceptor absorbance spectra were calculated in the presence and absence of Ca^{2+} (see Table 2). Förster critical distances, R_0, were calculated from the quantum yields (Q) and overlap integrals (J), assuming $\eta = 14$ and $\kappa^2 = 2/3$ (see Table 2). The frequency domain intensity decays of the labeled thin filaments were used to calculate fluorescence lifetimes. Representative fits for TnI Cys-117 in the presence and absence of Ca^{2+} are shown in Figure 3. The mean distances, R_{av}, obtained from these experiments (see Table 2) show that, in the thin filaments, TnI Cys-117 is ~8 Å further away from actin Cys-374 in the presence of Ca^{2+} than in the absence of Ca^{2+}, while the distance between TnI Cys-96 and actin Cys-374 is ~3.6 Å greater in the presence of Ca^{2+}. These results were further confirmed by steady-state fluorescence intensity measurements obtained while titrating the AEDANS-labeled Tn–Tm complex with either unlabeled actin or DABmal-labeled actin (data not shown).

DISCUSSION

Environment of TnI Cys-96 and Cys-117 in the Tn–Tm Complex and Reconstituted Thin Filaments.

Our lifetime-resolved anisotropy measurements and acrylamide quenching data indicate that the effects of Ca^{2+} on the environments of TnI Cys-96 and Cys-117 in the Tn–Tm complex differ from the effects in reconstituted thin filaments.

In the Tn–Tm complex, AEDANS labels on both Cys-96 and Cys-117 of TnI are less accessible to solvent (although the differences are relatively small) and less flexible in the presence of Ca^{2+}. These observations support the idea that the Cys-117 region of TnI interacts much more strongly with TnC in the presence of Ca^{2+} than in the absence of Ca^{2+} (1, 11, 12, 14). Our results are compatible with the recently reported (30) NMR solution structure of a complex of the N-terminal domain of cardiac TnC and the peptide fragment of residues 147–163 of cardiac TnI (equivalent to residues 115–131 of skeletal TnI), which showed that Ser-149 of cardiac TnI (equivalent to Cys-117 in our skeletal TnI mutant) is close to the N-terminal hydrophobic pocket of TnC.

Our results are also consistent with the observation that the N-terminal half of the inhibitory region of TnI, i.e., near Cys-96, interacts with TnC in a Ca^{2+}-dependent manner (8). The decreased flexibilities of the AEDANS labels in the presence of Ca^{2+} contrast with our previous distance distribution studies (13), which showed that the ternary Tn complex becomes much more flexible when Ca^{2+} binds to the regulatory sites of TnC. It is tempting to speculate that these differing observations may be due to a constraining effect of Tm in the Tn–Tm complex, but it must be kept in mind that large, Ca^{2+}-dependent fluctuations in the overall structure of Tn need not correlate with movements of individual fluorescence probes.

In the reconstituted thin filament, the effects of Ca^{2+} were different and more pronounced. For TnI Cys-96, the environment of the AEDANS fluorophore was not greatly affected by Ca^{2+}; its accessibility was unchanged, while its flexibility increased only moderately in the presence of Ca^{2+}. For TnI Cys-117, the AEDANS fluorophore was more accessible but less flexible in the presence of Ca^{2+}. Cys-96 and Cys-117 are both located in a region of TnI that interacts more closely with actin in the absence of Ca^{2+}, i.e., under conditions in which TnI inhibits actomyosin ATPase activity (6, 8). One might expect, therefore, to find that AEDANS labels on both of these residues would become more flexible as they move away from actin in the presence of Ca^{2+}. Instead, however, we found that there was a striking difference between TnI Cys-96 and Cys-117. There was a large Ca^{2+}-induced decrease in the flexibility of the AEDANS label on Cys-117, presumably due to tighter interaction of the Cys-117 region of TnI with TnC in the presence of Ca^{2+} (11, 12). On the other hand, there was a modest Ca^{2+}-induced increase in the flexibility of the AEDANS label on Cys-96. This probably reflects the fact that the region of TnI around Cys-96 binds much more tightly to actin in the absence of Ca^{2+} than it does to TnC in the presence of Ca^{2+} (8).

It is also interesting to consider the effect of actin on the flexibilities of the AEDANS labels attached to TnI by comparing the $r(0)$ values (see Table 1) obtained in the Tn–Tm complexes with those obtained in the reconstituted thin filaments. TnI Cys-96 does not interact with actin in the presence of Ca^{2+} (8), so it is not surprising to find that the flexibility of its AEDANS label in the presence of Ca^{2+} is the same in both the Tn–Tm complex and thin filaments. On the other hand, TnI Cys-96 does interact with actin in the absence of Ca^{2+} (8), causing the flexibility of the AEDANS label on Cys-96 to be much lower in the thin filaments than in the Tn–Tm complex. For TnI Cys-117, the flexibility of the AEDANS label is always lower in the thin filaments than in the Tn–Tm complex, regardless of whether Ca^{2+} is present. Thus, even though TnI Cys-117 interacts tightly with the hydrophobic pocket in the N-terminal domain of TnC in the presence of Ca^{2+} (11, 12), actin appears to remain close enough to restrict the mobility of the AEDANS label.

Ca^{2+}-Induced Movement of the Inhibitory Region of TnI in the Reconstituted Thin Filament.

In our calculations of R_0, we assumed $\kappa^2 = ⅔$, as it would be if both donor and acceptor dipoles rotated randomly and rapidly compared to the time scale of energy transfer (27, 31, 32). Limiting anisotropy values, $r(0)$ (see Table 1), indicate that AEDANS at TnI Cys-117 in the thin filament is relatively rigid in the presence of Ca^{2+}. We used θ values (Table 1), the half-angle of the cone within which AEDANS rotates rapidly, to calculate R_{min} and R_{max}

(Table 2) according to the method described by Stryer (32). It can be seen that the actual R_{av} values determined by energy transfer measurements have some degree of uncertainty. In practice, however, the range of distances should be smaller because this method for obtaining R_{min} and R_{max} assumes no rotational freedom of the energy acceptor and a unique direction of the polarization transitions (32, 33). For example, intermonomer or intra-monomer distances that were estimated by energy transfer measurements within actin based on the assumption that $\kappa^2 = 2/3$ showed reasonable agreement with distances obtained by X-ray diffraction data (34, 35).

The average distances R_{av}, obtained by assuming $\kappa^2 = 2/3$, between AEDANS at TnI Cys-117 and DABmal at actin Cys-374 in the reconstituted thin filaments were calculated to be 35.2 Å in the absence of Ca^{2+} and 43.3 Å in the presence of Ca^{2+}. Thus, TnI Cys-117 moves away from actin by ~8 Å when Ca^{2+} binds to the regulatory sites of TnC. Previously, another TnI amino acid residue, Cys-133, was found to move away from actin Cys-374 by 15 Å (36) and away from the nucleotide binding site and Gln-41 of actin by up to 9–10 Å (37), as a result of Ca^{2+} binding to the regulatory sites of TnC. The importance of the Cys-133 region of TnI was also suggested by sequence comparisons (38). Later, our cross-linking studies showed that in binary TnC–TnI complexes, Cys-117 and Cys-133 of TnI are close to Cys-57 and Cys-12, respectively, of mutant TnCs (39, 40). The crystal (9, 10, 41) and solution (42) structures of TnC show that residues 12 and 57 are located on opposite sides of the N-terminal, regulatory domain. Little is known about the three-dimensional structure of TnI, but the polypeptide segment between residues 117 and 133 binds to the hydrophobic pocket of TnC's N-terminal domain in the presence of Ca^{2+} (11). The data presented here now show that the Ca^{2+}-induced interaction of TnI with the N-terminal domain of TnC pulls both ends of the TnI segment of residues 117–133 away from actin.

We calculated the average distances between AEDANS at TnI Cys-96 and DABmal at actin Cys-374 in reconstituted thin filaments to be 40.2 and 43.8 Å in the absence and presence of Ca^{2+}, respectively. The difference, 3.6 Å, is relatively small, comparable for example to the distance (4–5 A) between residue 9 of TnI and the nucleotide-binding site or Gln-41 of actin (35). While TnI Cys-96, Cys-117, and Cys-133 all move away from actin Cys-374 when Ca^{2+} binds to the regulatory sites of TnC, the distances traversed by these residues increase as one proceeds toward the C-terminus of TnI along its polypeptide chain. The distance moved by Cys-96 is less than half of that moved by Cys-117 and less than one-fourth of the distance moved by Cys-133. This suggests the existence of a flexible "hinge" region near residue 96 in the middle of the TnI polypeptide chain, which would allow amino acid residues in the N-terminal half of TnI to interact with TnC in a Ca^{2+}-independent manner, while residues in the C-terminal half of TnI bind to actin in the absence of Ca^{2+} or to TnC in the presence of Ca^{2+}. The existence of such a flexible hinge region in TnI would help to explain large structural changes in TnI which occur when Ca^{2+} binds to the regulatory sites of TnC, as recently detected by neutron scattering of the TnC–TnI complex (43). This is illustrated in Figure 4.

In recent years, it has been demonstrated that muscle thin filaments exist in an equilibrium among three states: "blocked", "closed", and "open" (44). A thin filament in the blocked state cannot bind myosin. In the closed state, the thin filament binds myosin only weakly.

Myosin binds strongly to an open state thin filament and undergoes structural changes which accelerate its ATPase activity. Ca^{2+} regulates the equilibrium between these three states of the thin filament. In the absence of Ca^{2+}, the thin filament exists predominantly in a blocked state, and the inhibitory region of TnI interacts with actin. under these conditions, the thin filament remains relatively rigid (20, 45, 46). When Ca^{2+} binds to the regulatory sites of TnC, a hydrophobic pocket appears in its N-terminal, regulatory domain and interacts with a segment of TnI (residues 115–131) which overlaps with the C-terminal part of the inhibitory region (11, 12). These structural transitions also create new interactions between TnT and acidic residues in the N-terminal domain of TnC (47). Then the C-terminal half of TnI moves away from actin (36, 37). The N-terminal region of TnI, on the other hand, does not move to any great extent relative to actin and TnC when Ca^{2+} binds to the regulatory sites of TnC (48). The crystal structure of TnC in complex with an N-terminal peptide (residues 1–47) of TnI shows the TnI peptide binding to both the N- and C-terminal domains of TnC (49). It seems unlikely, therefore, that Ca^{2+}-dependent movement of the C-terminal region, but not the N-terminal region, of TnI would be accompanied by any significant movement of TnC away from actin.

In summary, we used AEDANS-labeled Cys-96 and Cys-117 of mutant TnIs to characterize Ca^{2+}-dependent changes in the structure and environment of the inhibitory region of TnI in the Tn–Tm complex and in reconstituted thin filaments. This is the first report to demonstrate structural movement of the inhibitory region of TnI in the thin filament. In the presence of Ca^{2+} and the absence of strongly bound myosin, the thin filament exists predominantly in a closed state. As noted by Squire and Morris (5), the closed state of the thin filament may reflect an intermediate position of the equilibrium between the blocked and open states rather than a distinct state. We are currently investigating the effect not only of Ca^{2+} but also of myosin S-1 on distances and distance distributions between actin filaments and the inhibitory region of TnI. These studies should shed additional light on the structural transitions that occur within thin filament proteins going from the closed to the open state.

ACKNOWLEDGMENT

We thank Masao Miki for his helpful advice.

This work was supported by Grant R01-AR-41161 from the National Institute of Arthritis and Musculoskeletal and Skin Diseases, National Institutes of Health, and by a grant to the Center for Fluorescence Spectroscopy (NIH RR-08119).

REFERENCES

1. Leavis PC, and Gergely J. (1984) CRC Crit. Rev. Biochem 16, 235–305. [PubMed: 6383715]
2. Zot A, and Potter JD (1987) Annu. Rev. Biophys. Biophys. Chem 16, 535–559. [PubMed: 2954560]
3. Farah C, and Reinach FC (1995) FASEB J. 9, 755–767. [PubMed: 7601340]
4. Tobacman LS (1996) Annu. Rev. Physiol 58, 447–481. [PubMed: 8815803]
5. Squire JM, and Morris EP (1998) FASEB J. 12, 761–771. [PubMed: 9657517]
6. Syska H, Wilkinson JM, Grand RJA, and Perry SV (1976) Biochem. J 153, 375–387. [PubMed: 179535]
7. Talbot JA, and Hodges RS (1981) J. Biol. Chem 256, 2798–2802. [PubMed: 6451620]

8. Grand RJA, Levine BA, and Perry SV (1982) Biochem. J 203, 61–68. [PubMed: 7103951]
9. Herzberg O, and James MNG (1985) Nature 313, 653–659. [PubMed: 3974698]
10. Sundaralingam M, Bergstrom R, Strasburg G, Rao ST, Roychowdhury P, Greaser M, and Wang BC (1985) Science 227, 945–948. [PubMed: 3969570]
11. McKay RT, Tripet BP, Hodges RS, and Sykes BD (1997) J. Biol. Chem 272, 28494–28500.
12. Tripet B, Van Eyk J, and Hodges RS (1997) J. Mol. Biol 271, 728–750. [PubMed: 9299323]
13. Zhao X, Kobayashi T, Malak H, Gryczynski I, Lakowicz JR, Wade R, and Collins JH (1995) J. Biol. Chem 270. 15507–15514.
14. Kobayashi T, Zhao X, Wade R, and Collins JH (1999) Biochim. Biophys. Acta 1430, 214–221. [PubMed: 10082949]
15. Ebashi S, Wakabayashi T, and Ebashi F. (1971) J. Biochem 69, 441–445. [PubMed: 5550981]
16. Smillie LB (1982) Methods Enzymol. 85, 234–241. [PubMed: 6289041]
17. Spudich JA, and Watt S. (1971) J. Biol. Chem 246,4866–4871. [PubMed: 4254541]
18. Tao T, Lamkin M, and Lehrer SS (1983) Biochemistry 22, 3059–3066. [PubMed: 6224509]
19. Takeda S, Kobayashi T, Taniguchi H, Hayashi H, and Maeda Y. (1997) Eur. J. Biochem 246, 611–617. [PubMed: 9219516]
20. Isambert H, Venier P, Maggs AC, Fattoum A, Kassab R, Pantaloni D, and Carlier M-F (1995) J. Biol. Chem 270, 11437–11444.
21. Butters CA, Tobacman JB, and Tobacman LS (1997) J. Biol. Chem 272, 13196–13202. [PubMed: 9148936]
22. Lakowicz JR, and Weber G. (1980) Biophys. J 32, 591–601. [PubMed: 7248463]
23. Lakowicz JR, Maliwal BP, Cherek H, and Balter A. (1983) Biochemistry 22, 1741–1752. [PubMed: 6849881]
24. Eftink M. (1983) Biophys. J 43, 323–334. [PubMed: 6354292]
25. Lakowicz JR (1983) Principles of Fluorescence Spectroscopy, Plenum Press, New York.
26. Hudson EN, and Weber G. (1973) Biochemistry 12,4154–4161. [PubMed: 4745664]
27. Laczko G, Lakowicz JR, Gryczynski I, Gryczynski Z, and Malak H. (1990) Rev. Sci. Instrum 61, 2331–2337.
28. Eftink MR, and Ghiron CA (1976) Biochemistry 15, 672–680. [PubMed: 1252418]
29. Lamkin M, Tao T, and Lehrer SS (1983) Biochemistry 22, 3053–3058. [PubMed: 6224508]
30. Li MX, Spyracopoulous L, and Sykes BD (1999) Biochemistry 38, 8289–8298. [PubMed: 10387074]
31. Cheung HC (1991) in Topics in Fluorescence Spectroscopy (Lakowicz JR, Ed.) Vol. 2, pp 127–176, Plenum Press, New York.
32. Stryer L. (1978) Annu. Rev. Biochem 47, 819–846. [PubMed: 354506]
33. Haas EE, Katchalsky-Katzir E, and Steinberg IZ (1978) Biochemistry 17, 5064–5070. [PubMed: 718874]
34. dos Remedios CG, and Moens PDJ (1995) J. Struct. Biol 115, 175–185. [PubMed: 7577238]
35. Miki M, O'Donoghue SI, and dos Remedios CG (1992) J. Muscle Res. Cell Motil 13, 132–145. [PubMed: 1534564]
36. Tao T, Gong B-J, and Leavis PC (1990) Science 247, 1339–1341. [PubMed: 2138356]
37. Miki M. (1990) Eur. J. Biochem 187, 155–162. [PubMed: 2105212]
38. Kobayashi T, Takagi T, Konishi K, and Cox JA (1989) J. Biol. Chem 264, 1551–1557. [PubMed: 2912973]
39. Kobayashi T, Tao T, Grabarek Z, Gergely J, and Collins JH (1991) J. Biol. Chem 266, 13746–13751.
40. Kobayashi T, Tao T, Gergely J, and Collins JH (1994) J. Biol. Chem 269, 5725–5729. [PubMed: 8119911]
41. Houdusse A, Love ML, Dominguez R, Grabarek Z, and Cohen C. (1997) Structure 5, 1695–1711. [PubMed: 9438870]
42. Slupsky CM, and Sykes BD (1995) Biochemistry 34, 15953–15964.

43. Stone DB, Timmins PA, Schneider DK, Krylova I, Ramos CHI, Reinach FC, and Mendelson RA (1998) J. Mol. Biol 218, 689–704.
44. McKillop DFA, and Geeves MA (1993) Biophys. J 65, 693–701. [PubMed: 8218897]
45. Ishiwata S, and Fujime S. (1972) J. Mol. Biol 68, 511–522. [PubMed: 4672238]
46. Yanagida T, Nakase M, Nishiyama K, and Oosawa F. (1984) Nature 307, 58–60. [PubMed: 6537825]
47. Kobayashi T, Zhao X, Wade R, and Collins JH (1999) Biochemistry 38, 5386–5391. [PubMed: 10220325]
48. Miki M, Kobayashi T, Kimura H, Hagiwara A, Hai H, and Maeda Y. (1998) J. Biochem 123, 324–331. [PubMed: 9538210]
49. Vassylyev DG, Takeda S, Wakatsuki S, Maeda K, and Maeda Y. (1998) Proc. Natl. Acad. Sci. U.S.A 95,4847–4852. BI991903B [PubMed: 9560191]

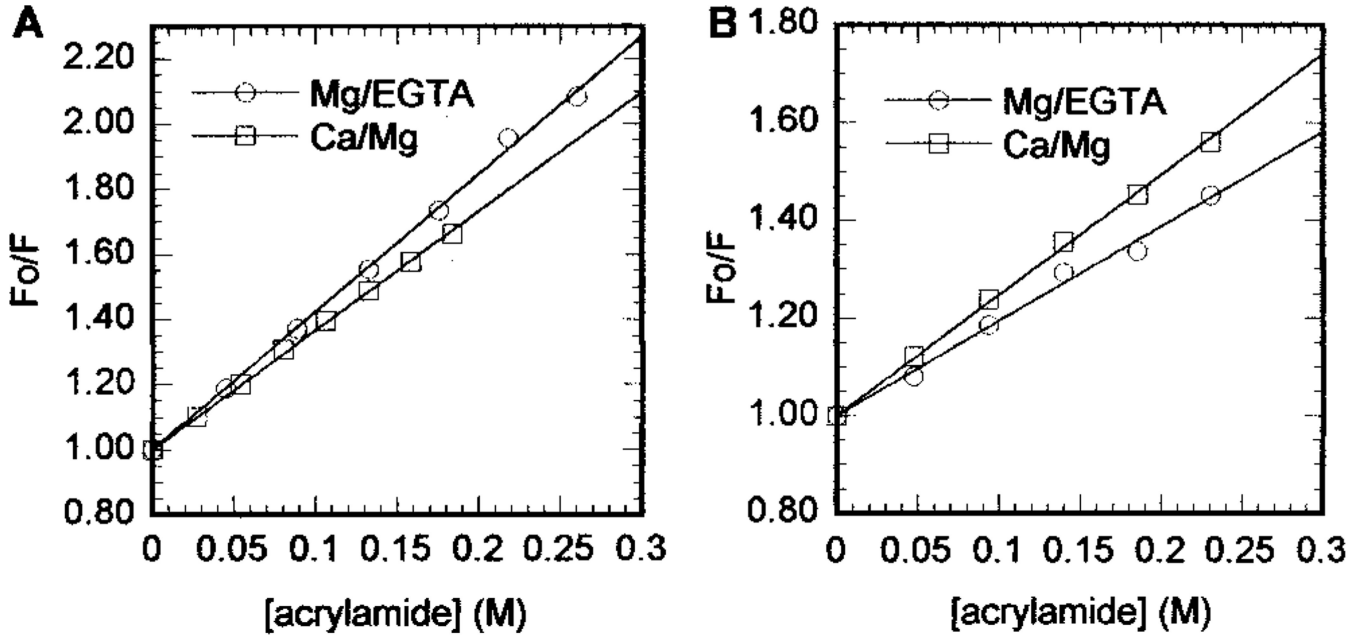

Figure 1:

Effect of Ca^{2+} on acrylamide quenching of AEDANS at TnI Cys-117: (A) Tn–Tm complex and (B) reconstituted thin filaments.

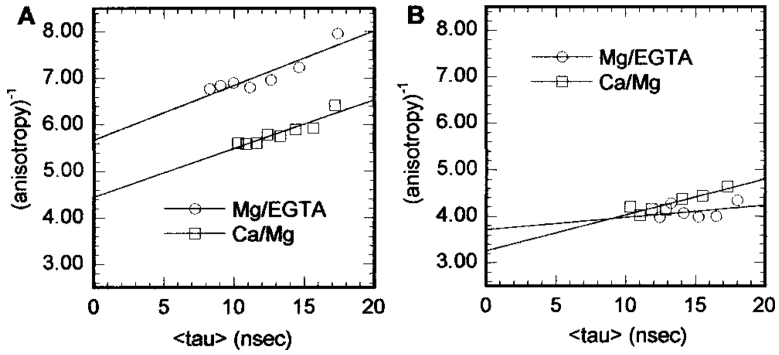

Figure 2:

Effects of Ca^{2+} on the lifetime-resolved anisotropy of AEDANS at TnI Cys-117: (A) Tn–Tm complex and (B) reconstituted thin filaments.

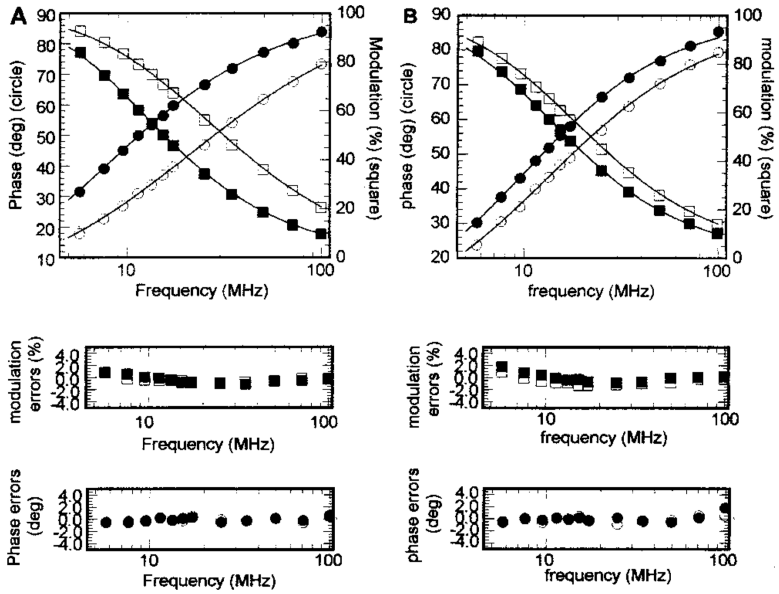

Figure 3:

Frequency domain phase and modulation data for AEDANS-labeled TnI Cys-117 in reconstituted thin filaments in the (A) absence of Ca^{2+} and (B) presence of Ca^{2+}: (black symbols) donor only and (white symbols) donor and acceptor. The phase angle increases and the modulation decreases as the frequency increases. In the presence of the acceptor, the lifetime decreases; thus, the frequency responses shift to higher frequencies. The solid lines are the best fitted curves for distance distribution analysis.

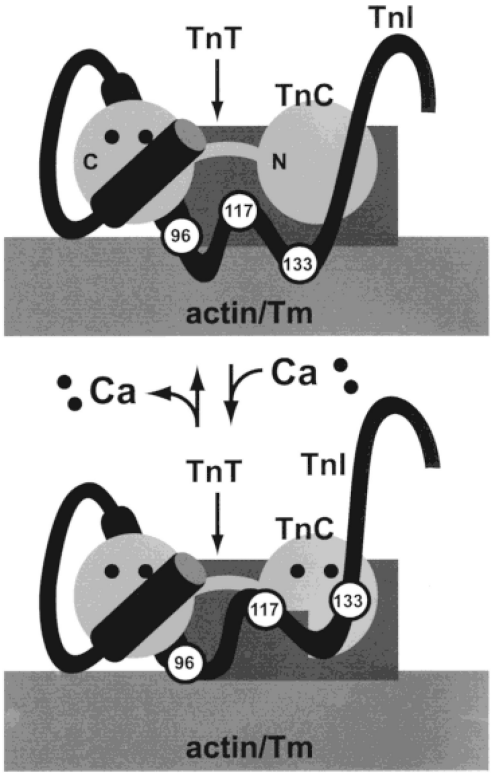

Figure 4:

Structural changes in TnI upon binding of Ca^{2+} to the regulatory sites of TnC. Schematic drawing illustrating a proposed Ca^{2+}-sensitive “hinge” near the middle of the TnI polypeptide chain. In the absence of Ca^{2+} (top), the inhibitory region (residues 96–117) and a second actin-binding site (region near residue 133) of TnI interact with actin–Tm. Binding of Ca^{2+} to the N-terminal, regulatory sites of TnC (bottom) exposes a hydrophobic pocket in TnC’s N-terminal domain. TnI residues 117–133 interact with the newly exposed hydrophobic pocket of TnC, moving the C-terminal part of TnI away from actin–Tm. The environment of the AEDANS label on TnI residue 96 does not change significantly when Ca^{2+} binds to the regulatory sites of TnC, but the side chain of the AEDANS label on TnI residue 117 becomes less flexible as it moves toward the hydrophobic pocket of TnC.

Table 1:

Fluorescence Quenching and Anisotropy of AEDANS–TnI

labeled position	complex	C^{2+}	K_{sv} (M^{-1})	$\langle\tau\rangle$ (ns)	$k_q \times 10^{-9}$ (M^{-1} s^{-1})	$r(0)$	θ (deg)
Cys-96	Tn–Tm	yes	4.3	15.5	0.28	0.234	26.5
		no	5.1	16.2	0.31	0.198	32.6
	thin filament	yes	4.3	15.1	0.28	0.234	26.5
		no	3.7	13.4	0.28	0.267	23.4
Cys-117	Tn–Tm	yes	3.7	17.2	0.21	0.225	29.2
		no	4.2	17.4	0.24	0.176	35.1
	thin filament	yes	2.6	17.3	0.15	0.337	9.1
		no	2.1	18.0	0.11	0.287	20.3

Table 2:

Distances between AEDANS–TnI and DABmal on Cys-374 of Actin in Reconstituted Thin Filaments[a]

labeled position	Ca^{2+}	Q	$J \times 10^{14}$(M^{-1} cm^{-1} mm^4)	$R_0(2/3)$ (Å)	R_{min} (Å)	R_{av} (Å)	R_{max} (Å)
Cys-96	yes	0.15	7.09	35.5	32.0	43.8	56.9
	no	0.14	7.01	35.0	28.1	40.2	52.6
Cys-117	yes	0.22	6.85	37.6	22.3	43.3	58.1
	no	0.25	7.03	38.7	23.6	35.2	46.4

[a] $R_0(2/3)$ is the Förster critical distance.